DOI: 10.1002/ejic.200800467

Synthesis of Single-Crystal Gold Nano- and Microprisms Using a Solvent-Reductant-Template Ionic Liquid

Yanan Gao,[a] Andreas Voigt,*[b] Min Zhou,[c] and Kai Sundmacher[a,b]

Keywords: Ionic liquids / Gold / Direct synthesis / Size control / Formation mechanism

A single-step procedure to obtain variable-sized nano- and microprisms of gold in ionic liquids is presented. Using an ionic liquid, 1-butyl-3-methylimidazolium hexafluorophosphate (bmimPF_6), as a solvent for the Au precursor as well as the reducing reagent for the reaction, one can control the size of the produced gold nanostructures. By varying the reaction time, prismatic particles with a very broad size range of 3–20 μm in diameter and 10–400 nm in thickness were obtained. Using an alternative ionic liquid, 1-butyl-3-methylimidazolium bis(trifluoromethanesulfonimide) (bmimTf_2N), uniform, single-crystal nano- and microprisms with an even larger size of about 100 μm in diameter were prepared. Large gold prisms of this type could be useful as a support for adsorbed species, as functional thin films, or as a conducting support for molecular electronics.

Introduction

Ionic liquids (ILs) are molten salts that are becoming increasingly important solvents due to their nonvolatility, thermal stability, and designable miscibility with cosolvents.[1] ILs have been widely used in various chemical reactions,[2] separations,[3] materials synthesis,[4] and electrochemical applications,[5] as well as a biopolymer[6] and in molecular self-assembly.[7] As alternative "green" solvents, the advantages of ILs in different material-synthesis processes have been realized and receive more and more attention. The synthesis of nanostructured materials, such as mesoporous materials,[4f,8] hollow microspheres,[9] CuCl nanoplatelets,[10] CoPt nanorods,[11] nanocrystalline metals,[12] and nanoporous platinum[13] in IL solvents/templates is already known. Recent work related to the preparation of nanomaterials in ILs has been reviewed.[14]

Recently, nanostructured gold has attracted much attention because of its unique physical and chemical properties, and its important applications in catalysis, photoelectronic devices, and biomedicine.[15] These properties and applications strongly depend on the morphology of the gold. However, the production of nanostructures by a shape-controlled procedure is still a challenge in the field of material design, and there is great interest in developing new methods for fabricating shape-controlled nanomaterials. Up to now, some gold nanostructures such as nanospheres,[16] nanowires,[17] nanorods,[18] nanodisks,[4e,19] nanorings,[20] nanoboxes,[21] nanocubes,[22] and branched nanocrystals,[23] have been routinely synthesized using various approaches. Moreover, 2D gold nanostructures with large surface areas have received considerable attention, mainly due to their potential applications in efficient surface-enhanced Raman scattering substrates,[24] as gas sensors,[25] and as ideal devices for photothermally triggered drug release in tissues.[15a] These nano- or micrometer-sized gold plates and prisms have been obtained by biological,[26] photochemical,[27] wet-chemical,[15c] and microwave[28] methods. However, general synthetic approaches of 2D gold materials involve the addition of various capping agents such as surfactants, polyols, surface-regulating polymers, polyaniline, and so on.[15a,15c,17,22,29] Up to now, a selective fabrication of uniform, shape-controlled 2D gold nanostructures without additional capping agents remains a challenge.

Herein we demonstrate a new and simple method for the preparation of uniform, shape-controlled single-crystal gold nano- and microprisms by a "green" route. No capping agents were needed, and a common water-immiscible "green" solvent IL, 1-butyl-3-methylimidazolium hexafluorophosphate (bmimPF_6), acted as both a solvent for the Au precursor and as reducing reagent for the reaction as well as a template to control the shape of Au nanostructures. An important process parameter was the reaction time as it affected the particle size significantly. The size of the pro-

[a] Max Planck Institute for Dynamics of Complex Technical Systems,
Sandtorstrasse 1, 39106 Magdeburg, Germany
[b] Process Systems Engineering, Otto von Guericke University Magdeburg,
Universitätsplatz 2, 39106 Magdeburg, Germany
Fax: +49-391-6110606
E-mail: Andreas.Voigt@VST.Uni-Magdeburg.de
[c] Analytical Chemistry, Ruhr-Universität Bochum,
Universitätsstr. 150, Gebäude NC/788, 44780 Bochum, Germany

Supporting information for this article is available on the WWW under http://www.eurjic.org or from the author.

duced prismatic gold particles could be controlled in a very broad range of 3–20 μm in width and 10–400 nm in thickness correspondingly.

Results and Discussion

Synthesis

In our process, a desired amount of gold precursor $HAuCl_4 \cdot 3H_2O$ was first dissolved in $bmimPF_6$, followed by the addition of small amounts of water. As $bmimPF_6$ and water are immiscible, the resulting solution phase separates, with the lower layer as the $bmimPF_6$-rich phase and the upper layer as the water phase. After vigorous agitation and equilibration at ambient temperature, the gold precursor $HAuCl_4 \cdot 3H_2O$ still resides in the lower $bmimPF_6$ phase, as indicated by the golden color of the lower part of the solution and the colorless solution in the upper part. The solution was kept at ambient temperature without stirring for 72 h. The formation of single-crystal Au nanostructures was visible by the appearance of solid gold particles. More and more Au material was obtained by prolonged reaction time. Higher process temperature (i.e., about 90 °C) remarkably accelerated the reaction process, and Au nano- and microprisms were obtained within tens of minutes up to a few hours. The process was mainly controlled by the concentration of $HAuCl_4 \cdot 3H_2O$ and by the temperature. The products were collected by centrifugation (10000 rpm) and repeatedly washed with acetone.[30]

Structural Characterization

A representative optical image of the synthesized gold nanostructures (process temperature T = 90 °C, process duration t = 4 h) shows the presence of a large number of triangular, hexagonal, and truncated triangular gold prisms with a smooth surface morphology (Figure 1). The number of nanoprisms is very high and is significantly higher than what has been reported earlier.[15a,15c,26a,26b,29c,29g,31] The average particle size is slightly less than 20 μm in diameter.

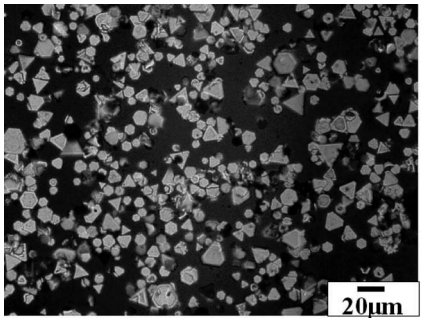

Figure 1. Optical microscopic image of the synthesized Au prisms obtained at t = 4 h and T = 90 °C.

A similar result was observed by scanning electron microscopy (SEM, see Figure 2). The gold nanoprisms exhibit sharp edges and a very narrow size distribution. Their surfaces are smooth with no obvious defects. AFM images of several samples obtained in different reaction time with a diameter between 3 and 20 μm indicate that the particles have a corresponding thickness from 10 to 400 nm (AFM image of a gold particle with a diameter of about 20 μm is shown in the Supporting Information). Powder XRD of the produced Au particles correspond to the well-known face-centered cubic (fcc) gold crystal structure (Figure 3). The relatively low diffraction intensity of the (200) and (220) planes compared with that of the (111) plane can be attributed to a preferential orientation of the (111) plane perpendicular to the supporting substrate. The (111) plane is in fact the hexagonal plane seen in the microscopy pictures. A typical transmission electron microscopy (TEM) image of a single Au nanohexagon and the corresponding electron

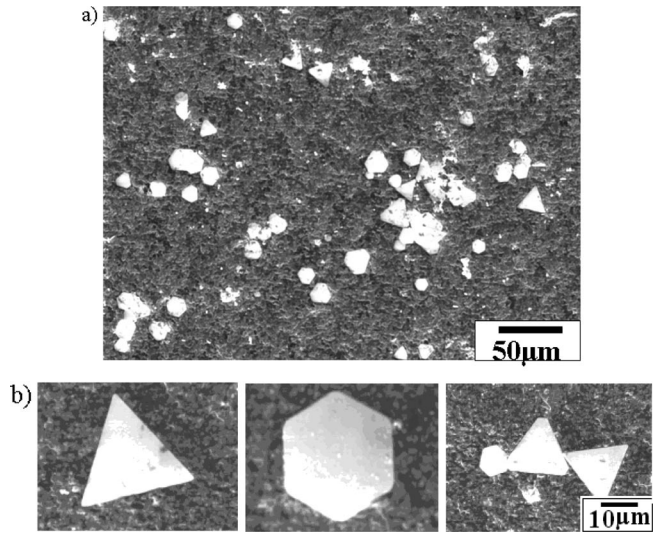

Figure 2. Low magnification (a) and high magnification (b) SEM images of the synthesized Au prisms obtained at t = 4 h and T = 90 °C.

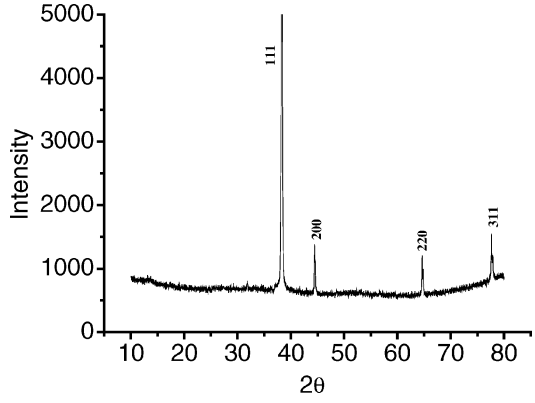

Figure 3. The X-ray diffraction pattern of Au particles with Miller indices at the corresponding intensity peaks (taken from the corresponding database).

diffraction pattern (SAED) are presented in Figure 4. The SAED pattern clearly shows that the particle is highly crystalline. The hexagonal nature of the diffraction points indicates again that the hexagonal gold nanoprisms are preferentially oriented with their (111) plane normal to the electron beam. The diffraction points could be indexed based on the fcc structure of gold. The presence of the 1/3{422} reflections (circled point) indicates that the surface of the gold hexagon is atomically flat.[32] Similar results were also obtained for nanoprisms with other shapes.

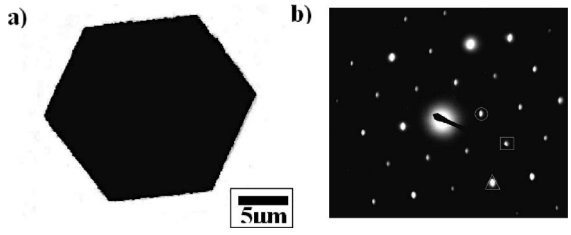

Figure 4. (a) TEM image of an individual gold hexagon prepared by t = 4 h and T = 90 °C. (b) SAED pattern of the gold hexagon in (a).

Formation Process

We will now discuss the structuring process based on the observations and results. We argue that the IL, bmimPF_6, plays a crucial role in the formation process of the gold nano- and microprisms. It has been mentioned already that $HAuCl_4 \cdot 3H_2O$ resides in the lower solution part, the IL phase, rather than in the upper aqueous phase. This means that bmimPF_6 first acts as a solvent for the reactant. The special interaction between bmimPF_6 and $AuCl_4^-$ may be attributed to the formation of carbine complexes through the C-2 of the bmimPF_6 cation and the metal ions.[33] Also, extended hydrogen bonding between the chlorine atoms of $AuCl_4^-$ and C–H and N–CH_2 protons of the imidazolium ring may lead to the enrichment of $AuCl_4^-$ in bmimPF_6.[34] The residence of $AuCl_4^-$ in such an IL environment provides the possibility of reducing $AuCl_4^-$ into gold atoms, as it is well known that $HAuCl_4 \cdot 3H_2O$ is stable in water without any reducing agents even at a high temperature of 90 °C (the decomposition temperature of $HAuCl_4 \cdot 3H_2O$ is about 150 °C). Therefore, one can assume that bmimPF_6 acts as a reducing agent in the formation process of the Au nanoparticles. The reducing character of bmimPF_6 can be related to the C=C olefinic bonds of the imidazolium cation. FTIR spectra of pure bmimPF_6 and oxidized bmimPF_6[35] are presented in the Supporting Information. It shows that the C–H stretching vibration of the imidazolium ring (which appears at 3172 and 3126 cm^{-1}) shifts to 3150 and 3092 cm^{-1}, respectively. The bands at 2967, 2940, and 2878 cm^{-1} [corresponding to the CH_3(N) and CH_2 stretching vibrations] move to 2960, 2935, and 2873 cm^{-1}, respectively. The bands at 1575 and 1467 cm^{-1} (corresponding to the imidazolium ring stretching and the CH_2 and CH_3 bend vibrations) shift to 1571 and 1463 cm^{-1}, respectively. These changes demonstrate that there are strong interactions between the imidazolium cation, $bmim^+$, and the $AuCl_4^-$ anion.[27c] In addition, a few new bands appear after the oxidation of bmimPF_6. The peaks at 3120 and 1061 cm^{-1} indicate the formation of a C–OH group. The peaks at 1525, 1452, and 1371 cm^{-1} suggest the appearance of a carboxyl group. Further, the appearance of two new bands at 1300 and 1250 cm^{-1} can be related to the formation of epoxide compounds. From these results, we can see that the C=C olefinic bond of bmimPF_6 was gradually oxidized into an epoxide, alcohol, and finally to a ketone by $AuCl_4^-$ in the presence of water. The existence of an oxygen element was confirmed by EDS spectroscopy (see Supporting Information). The resulting ketone can be absorbed onto the surface of the Au particles as a capping agent and therefore guide the formation of Au prisms (as discussed later). Our contrast experiment revealed that Au nano- and microstructures were only obtained in the presence of water, indicating that H_2O is indispensable for the reduction of $AuCl_4^-$. Although water and hydrophobic bmimPF_6 are immiscible, a certain amount of water can still be partitioned into hydrophobic ILs phase because of special interactions between water and ILs.[36] Water has been shown to have a great effect on the structural organization of ILs and thus the outcome of chemical reactions.[37] In our case, the redox reaction between $AuCl_4^-$ and bmimPF_6 may occur according to Equation (1).

The formation mechanism of the gold nano- and microprisms in the $AuCl_4^-$-bmimPF_6 reaction medium was investigated by monitoring the growth process of gold nanoparticles. Optical microscopy was chosen because it can be used to directly observe gold particles in a solution state, thus avoiding the particle aggregation induced by vacuum when measured through SEM or TEM. Optical microscopic images can be correlated with the time-dependent spectroscopic observations and they reveal that the initial tiny Au particles were gradually converted to prismatic structures as triangles, hexagons, and truncated triangles (see Figure 5). At a very early stage of the process (10 min), small irregular-shaped gold particles had already formed because of the initial reduction of $AuCl_4^-$ by bmimPF_6 (Figure 5a). These tiny gold particles aggregated into relatively larger nanostructures, which then gradually evolved into a quasiprismatic structure and finally formed crystal-

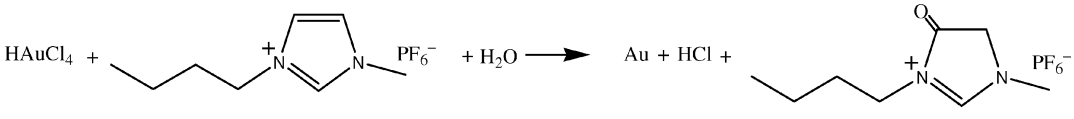

(1)

line nano- and microprisms. The size and number of gold nano- and microprisms increased with time, accompanied by a corresponding decrease in the number of Au nanoparticles (Figures 5b and c). After 2.5 h of reaction time, the gold particles almost completely disappeared and were converted into the Au microprisms. The size of the Au prisms reached more than 10 μm after 4 h of reaction time (Figure 5d). The transformation of tiny nanoparticles into larger aggregates and into prismatic Au or Ag structures with time was also observed by other groups.[26a,29a,32] Mirkin et al. reported the light-induced conversion of aggregated silver nanoparticles into larger triangular nanoprisms. They proposed that once the spherical Ag nanoparticles and small nanoclusters are consumed, the reaction terminates.[32] However, it is of particular interest that our resultant regular-shaped single-crystal Au nano- and microprisms still successively grew with reaction time in the IL-based process. Figure 6 shows that the relatively small Au prisms possess a regular-shaped structure with a smooth surface (2.5 h of reaction time). The regular shape of the structure was always maintained during the successive growth of our Au nanoprisms (2.5–4.5 h of reaction time). Hence, it is evident that the planar size of single-crystal gold nanoprisms can be well adjusted by controlling the reaction time of this process. Our process is therefore the first example where a size control for single-crystal gold nanoprisms was achieved over such a large range from 3 μm up to 20 μm. We believe that both the weak reducing ability of $bmimPF_6$ and the formation of carbine complexes or hydrogen bonding between $bmimPF_6$ and $AuCl_4^-$ would lead to the slow reaction of $AuCl_4^-$ with $bmimPF_6$; Au atoms can thus be continuously provided by the reduction of unreacted $AuCl_4^-$. As a result, the initial gold nanoprisms may act as seeds and gradually grow by incorporating these Au atoms.

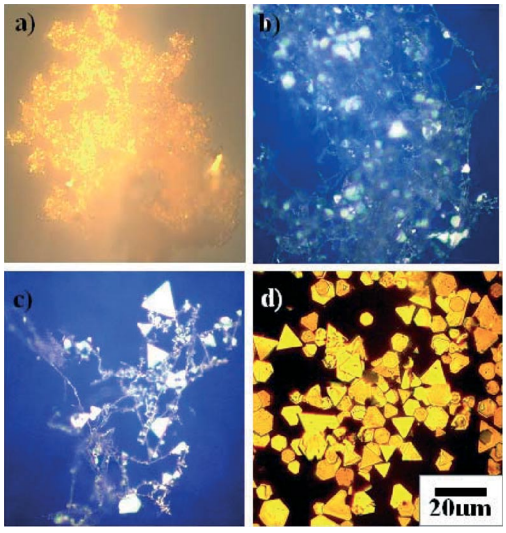

Figure 5. Optical microscopic images illustrating the morphology changes during the reaction. After 10 min (a), 30 min (b), 1 h (c), and 4 h (d) of reaction time. The scale bar is 20 μm for all images.

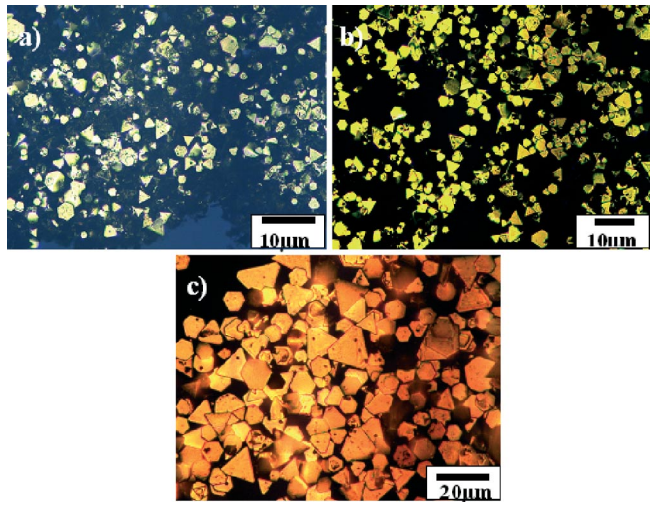

Figure 6. Optical microscopic images illustrating the morphology changes after 2.5 h (a), 3.5 h (b), and 4.5 h (c) reaction time.

Influence of Ionic Liquid Type on Nanoparticle Aggregation

It is worth mentioning that the aggregation behavior of the tiny gold nanoparticles was also important for their further growth into single-crystal Au nano- and microprisms. A recent study on the biological synthesis of triangular gold nanoprisms revealed that single-crystalline gold nanoprisms evolve from aggregated nanoparticles. The tiny nanoparticles are in close contact and sinter into "liquid-like" spherical gold nanoparticles. This process is followed by transformation to a quasitriangular shape and subsequent formation of crystalline nanoprisms.[26a] Moreover, the aggregation and fusion of small gold nanostructures and their further evolution into large single-crystal nanoplates were also observed by a more recent study.[29a] In our work, optical microscopy clearly indicates that the tiny gold particles are inclined to aggregate together in the $bmimPF_6$-rich phase and the single-crystal Au nano- and microprisms gradually evolve from these small gold particles. In contrast, Au nano- and microprisms were not obtained in two other hydrophilic ILs, 1-butyl-3-methylimidazolium chloride (bmimCl) and 1-butyl-3-methylimidazolium tetrafluoroborate ($bmimBF_4$). They probably can not provide such an aggregation environment for these tiny gold particles. To prove that the aggregation behavior is necessary when using a different imidazolium-type hydrophobic IL, we applied the same procedure to another common hydrophobic IL, 1-butyl-3-methylimidazolium bis(trifluoromethanesulfonimide) ($bmimTf_2N$). Similarly, the uniform, single-crystal gold nano- and microprisms were obtained, but with an even larger size of about 100 μm in diameter (Figure 7). Such large regular-shaped Au prisms have scarcely been reported. The large gold surface area can be used as a support for adsorbed species, as functional thin film in thiol chemistry and scanning probe microscopes (SPMs) for imaging or force measurements, as well as a conducting support for molecular electronics studies.[38]

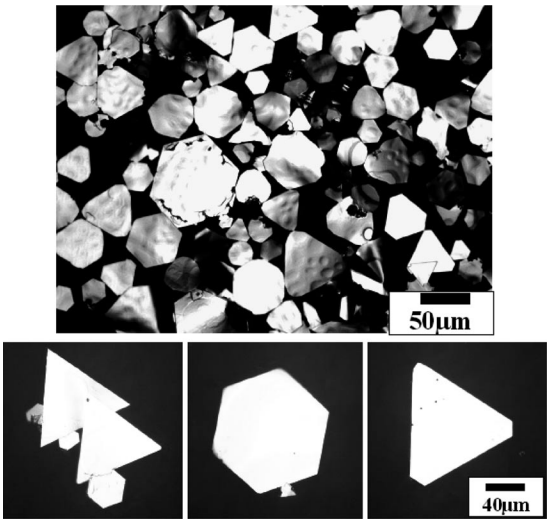

Figure 7. Optical microscopic images of synthesized Au prisms obtained in a bmimTf_2N-based process at t = 4 h and T = 90 °C.

Transfer Process from Aqueous Phase to IL

The phase transfer of Au nanoparticles from an aqueous phase to a bmimPF_6 solution was recently reported.[39] The alcohol-like polarity and ionic properties of bmimPF_6 are considered to result in this particular transfer process.[39] The aggregation behavior of Au nanoparticles was also observed after the phase transfer; however, one should mention that the Au nanoparticle morphology was preserved,[39] which is remarkably different from our observation that single-crystal Au nano- and microprisms were converted from the Au nanoparticle aggregates. We compared the two different systems and discovered that in the recent report, gold nanoparticles were first prepared upon reduction of a $HAuCl_4$ aqueous solution with citrate, but there were no additional capping agents added to the system. However, we obtained our gold nano- and microstructures by the reduction of $AuCl_4^-$ with bmimPF_6. It is thus reasonable to expect that the oxidation product of bmimPF_6 is also a key to produce the Au nano- and microprisms. We suggest that the resulting oxide serves as a capping agent and acts as a kinetic control of the growth rates of various faces of the Au nanoparticles by selectively adsorbing onto different crystallographic planes. This leads finally to the formation of large single-crystal Au nano- and microprisms. Although the synthesis of Au nano- and microprisms has been widely proposed, capping agents like polyvinylpyrrolidone,[15a,22,29e,29f,40] polystyrene-*block*-poly(2-vinylpyridine),[41] actone,[31a] lemongrass,[26a,31d] α-D-glucose,[42] proteins,[29c] salicylic acid,[31b] aspartate,[26b] trisodium citrate,[43] tartaric acid,[31c] or ascorbic acid[44] are generally necessary. A common feature of these capping agents is the existence of a ketone group in these aldehydes, ketones, and carboxylic acids. The oxidation product of bmimPF_6 is essentially a ketone, which therefore allows us to consider that the obtained ketone actually plays the same role as the typical capping agents. The carbonyl oxygen atom of the capping agent can interact with the gold atoms of the gold clusters by forming a backbond. This leads to a significant flattening of the Au nanoparticles, and the surface Au–Au bond will break as a result of the adsorption of the ketone molecules.[45] The growth rates of different faces of the Au particles are thus kinetically controlled, which is reflected by a rapid growth along the {111} direction and a relatively slow growth along the {100} face. As a consequence, planar single-crystal Au nano- and microstructures were formed. Moreover, because of the adsorption of the ketone molecules, the rearrangement of the surface Au atoms[45] will restructure the gold nanoparticle surface to "liquid-like" and activate it. This is also favorable for the observed sintering of tiny Au nanoparticles into the aggregated Au nano- and microstructures.

The whole formation process of Au nano- and microprisms in bmimPF_6 can be proposed as illustrated in Scheme 1. The tiny Au particles are first formed by the reduction of $AuCl_4^-$ with bmimPF_6. These Au nanoparticles aggregate in the bmimPF_6-rich phase and by absorption of the oxidation product of bmimPF_6, small gold particles with a "liquid-like" surface are created. These "fluffy" Au particles sinter into small single-crystal prismatic nanostructures. The resulting small Au prisms successively grow by incorporating Au atoms which are provided by the slow

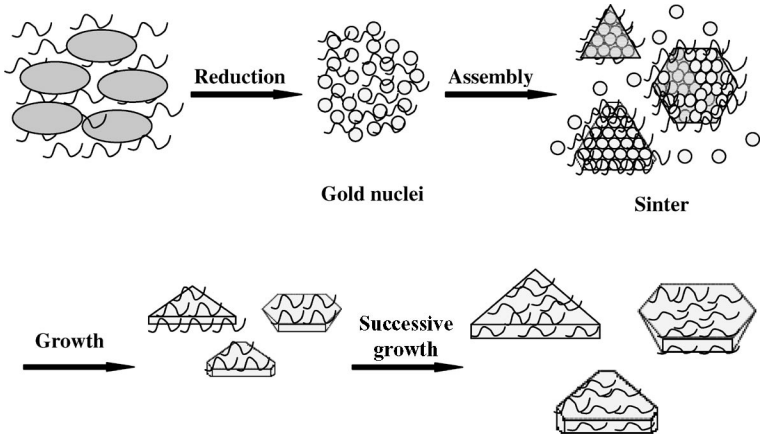

Scheme 1. Schematic illustration of the formation of gold nano- and microprisms in the hydrophobic IL solutions.

reduction of unreacted $AuCl_4^-$. The growth rate of the {111} face is higher than that of the other faces because of the adsorption of the ketone molecules on those surfaces. Finally, large single-crystal Au nano- and microprisms are obtained.

Conclusions

We have demonstrated that hydrophobic ILs can be employed as a new and alternative medium to prepare regular-shaped single-crystal Au nano- and microprisms without the need for additional capping agents. The hydrophobic ILs act as multifunctional molecules, that is, as a solvent for the Au precursor, as a reducing agent for the reaction, and as a template for the direct formation of single-crystal Au prisms. Therefore, this work offers a significant new and simple "green" route for selective synthesis of uniform single-crystal Au nano- and microprisms. Moreover, the particle size of Au nano- and microprisms can be well controlled in a very large range by controlling the reaction time. The presented synthesis procedure may be a versatile approach that can be extended to fabricate other interesting metal nanomaterials like specific catalysts or biosensor material.

Experimental Section

In a typical synthesis, $HAuCl_4 \cdot 3H_2O$ (0.03 g) was dissolved in water (1.0 g). The aqueous gold precursor solution was then mixed with $bmimPF_6$ (3.0 g). The two phases separated into two layers: the lower golden $bmimPF_6$-rich phase and the upper colorless water phase, that is, $HAuCl_4 \cdot 3H_2O$ was extracted into the $bmimPF_6$ phase. The two-phase solution was kept at ambient temperature without stirring for 72 h. Solid yellow particles were observed by visual inspection. The amount of material increased with prolonged reaction time. An additional experiment at a higher temperature of 90 °C was carried out where, by visual inspection, yellow particles were observed after 10 min and after up to a few hours. The solid particle products were separated from the solution by centrifugation with 10000 rpm. For additional analysis by microscopy, TEM, and XRD, the gold particles were repeatedly washed with acetone.[30] The microscopic pictures were taken with a Zeiss Axio Imager.A1 supplemented with an AxioCam digital camera. The TEM pictures were obtained with a JEM-100CX II (JEOL) at 100 kV acceleration where the washed particles were placed on a copper-carbon grid. The XRD data were obtained with the powder diffractometer X'Pert Pro from PANalytical B.V. (Cu-K_α radiation, λ = 0.154 Å) by placing small traces of particles on a silica wafer. SEM pictures were taken from nonsputtered samples placed on carbon holders. AFM measurements were performed using a Nanoscope IIIa Multimode AFM (Digital Instruments Inc., USA) at 25 °C, utilizing a silicon cantilever with a resonance frequency about 200 kHz in tapping mode at a scan rate of 0.5 Hz. The samples were prepared by applying a drop of solution (approximately 1 mL) on a freshly cleaved mica surface and drying it in air. FTIR data were taken with a Nicolet 6700 from Thermo Electron Corporation from small amounts of the ionic liquid solution before and after the reaction.

Supporting Information (see footnote on the first page of this article): AFM image of a single hexagonal Au prism prepared in $bmimPF_6$ at t = 4 h and T = 90 °C (Figure S1), EDS of a Au prism obtained in $bmimPF_6$ (Figure S2), and FTIR spectroscopic data of $bmimPF_6$ and the oxidized $bmimPF_6$ after reaction (Figure S3).

Acknowledgments

Y. G. acknowledges his postdoctoral fellowship from the Max Planck society. The authors thank Bianka Stein, Markus Ikert, Wei Xu, Christian Fuchs, and Evelin Felsch for their assistance throughout the work.

[1] a) A. Kumar, S. Murugesan, V. Pushparaj, J. Xie, C. Soldano, G. John, O. Nalamasu, P. M. Ajayan, R. J. Linhardt, *Small* **2007**, *3*, 429–433; b) T. Welton, *Chem. Rev.* **1999**, *99*, 2071–2083.
[2] a) C. C. Cassol, A. P. Umpierre, G. Machado, S. I. Wolke, J. Dupont, *J. Am. Chem. Soc.* **2005**, *127*, 3298–3299; b) W. Leitner, *Nature* **2003**, *423*, 930–931.
[3] A. Arce, M. J. Earle, H. Rodriguez, K. R. Seddon, *J. Phys. Chem. B* **2007**, *111*, 4732–4736.
[4] a) M. A. Gelesky, A. P. Umpierre, G. Machado, R. R. B. Correia, W. C. Magno, J. Morais, G. Ebeling, J. Dupont, *J. Am. Chem. Soc.* **2005**, *127*, 4588–4589; b) E. R. Cooper, C. D. Andrews, P. S. Wheatley, P. B. Webb, P. Wormald, R. E. Morris, *Nature* **2004**, *430*, 1012–1016; c) S. D. Miao, Z. M. Liu, B. X. Han, J. Huang, Z. Y. Sun, J. L. Zhang, T. Jiang, *Angew. Chem. Int. Ed.* **2006**, *45*, 266–269; d) B. G. Trewyn, C. M. Whitman, V. S. Y. Lin, *Nano Lett.* **2004**, *4*, 2139–2143; e) T. K. Sau, C. J. Murphy, *J. Am. Chem. Soc.* **2004**, *126*, 8648–8649; f) Y. Zhou, M. Antonietti, *J. Am. Chem. Soc.* **2003**, *125*, 14960–14961; g) Y. Zhou, J. H. Schattka, M. Antonietti, *Nano Lett.* **2004**, *4*, 477–481; h) K. Kim, D. Demberelnyamba, H. Lee, *Langmuir* **2004**, *20*, 556–560.
[5] E. V. Dickinson, M. E. Williams, S. M. Hendrickson, H. Masui, R. W. Murray, *J. Am. Chem. Soc.* **1999**, *121*, 613–616.
[6] N. Kimizuka, T. Nakashima, *Langmuir* **2001**, *17*, 6759–6761.
[7] a) Y. He, T. P. Lodge, *J. Am. Chem. Soc.* **2006**, *128*, 12666–12667; b) Y. He, P. Simone, Z. Li, T. P. Lodge, *J. Am. Chem. Soc.* **2006**, *128*, 2745–2750; c) Y. A. Gao, Z. H. Li, J. M. Du, B. X. Han, G. Z. Li, W. G. Hou, D. Shen, L. Q. Zheng, G. Y. Zhang, *Chem. Eur. J.* **2005**, *11*, 5875–5880; d) Y. A. Gao, X. Y. Zhao, B. Dong, L. Q. Zheng, N. Li, S. H. Zhang, *J. Phys. Chem. B* **2006**, *110*, 8576–8581.
[8] Y. Zhou, M. Antonietti, *Adv. Mater.* **2003**, *15*, 1452–1455.
[9] T. Nakashima, N. Kimizuka, *J. Am. Chem. Soc.* **2003**, *125*, 6386–6387.
[10] A. Taubert, *Angew. Chem. Int. Ed.* **2004**, *43*, 5380–5382.
[11] Y. Wang, H. Yang, *J. Am. Chem. Soc.* **2005**, *127*, 5316–5317.
[12] a) C. L. Aravinda, W. Freyland, *Chem. Commun.* **2004**, 2754–2755; b) F. Endres, M. Bukowski, R. Hempelmann, H. Natter, *Angew. Chem. Int. Ed.* **2003**, *42*, 3428–3430; c) G. Bühler, C. Feldmann, *Angew. Chem. Int. Ed.* **2006**, *45*, 4864–4867.
[13] J. F. Huang, I. W. Sun, *Chem. Mater.* **2004**, *16*, 1829–1831.
[14] a) A. Taubert, Z. H. Li, *Dalton Trans.* **2007**, 723–727; b) P. Migowski, J. Dupont, *Chem. Eur. J.* **2007**, *13*, 32–39.
[15] a) C. C. Li, W. P. Cai, B. Q. Cao, F. Q. Sun, Y. Li, C. X. Kan, L. D. Zhang, *Adv. Funct. Mater.* **2006**, *16*, 83–90; b) M. C. Daniel, D. Astruc, *Chem. Rev.* **2004**, *104*, 293–346; c) X. P. Sun, S. J. Dong, E. K. Wang, *Angew. Chem. Int. Ed.* **2004**, *43*, 6360–6363.
[16] a) J. Liu, S. Mendoza, E. Roman, M. J. Lynn, R. Xu, A. E. Kaifer, *J. Am. Chem. Soc.* **1999**, *121*, 4304–4305; b) P. Raveendran, J. Fu, S. L. Wallen, *Green Chem.* **2006**, *8*, 34–38.
[17] J. U. Kim, S. H. Cha, K. Shin, J. Y. Jho, J. C. Lee, *Adv. Mater.* **2004**, *16*, 459–464.
[18] a) F. Kim, J. H. Song, P. D. Yang, *J. Am. Chem. Soc.* **2002**, *124*, 14316–14317; b) J. Murphy, N. R. Jana, *Adv. Mater.* **2002**, *14*, 80–82; c) B. D. Busbee, S. O. Obare, C. J. Murphy, *Adv. Mater.*

2003, *15*, 414–416; d) N. R. Jana, L. Gearheart, C. J. Murphy, *J. Phys. Chem. B* **2001**, *105*, 4065–4067.
[19] Y. Zhou, C. Y. Wang, Y. R. Zhu, Z. Y. Chen, *Chem. Mater.* **1999**, *11*, 2310–2312.
[20] a) Y. G. Sun, Y. N. Xia, *Adv. Mater.* **2003**, *15*, 695–699; b) G. S. Metraux, Y. C. Cao, R. C. Jin, C. A. Mirkin, *Nano Lett.* **2003**, *3*, 519–522.
[21] a) Y. G. Sun, Y. N. Xia, *Science* **2002**, *298*, 2176–2179; b) Y. G. Sun, Y. N. Xia, *J. Am. Chem. Soc.* **2004**, *126*, 3892–3901.
[22] F. Kim, S. Connor, H. Song, T. Kuykendall, P. D. Yang, *Angew. Chem. Int. Ed.* **2004**, *43*, 3673–3677.
[23] a) S. H. Chen, Z. L. Wang, J. Ballato, S. H. Foulger, D. L. Carroll, *J. Am. Chem. Soc.* **2003**, *125*, 16186–16187; b) E. Hao, R. C. Bailey, G. C. Schatz, J. T. Hupp, S. Y. Li, *Nano Lett.* **2004**, *4*, 327–330.
[24] B. Ren, G. Picardi, B. Pettinger, R. Schuster, G. Ertl, *Angew. Chem. Int. Ed.* **2005**, *44*, 139–142.
[25] J. J. Mcnerey, P. R. Buseck, R. C. Hanson, *Science* **1972**, *178*, 611–612.
[26] a) S. S. Shankar, A. Rai, B. Ankamwar, A. Singh, A. Ahmad, M. Sastry, *Nat. Mater.* **2004**, *3*, 482–488; b) Y. Shao, Y. D. Jin, S. J. Dong, *Chem. Commun.* **2004**, 1104–1105; c) S. P. Chandran, M. Chaudhary, R. Pasricha, A. Ahmad, M. Sastry, *Biotechnol. Prog.* **2006**, *22*, 577–583; d) A. Rai, A. Singh, A. Ahmad, M. Sastry, *Langmuir* **2006**, *22*, 736–741.
[27] a) D. Ibano, Y. Yokota, T. Tominaga, *Chem. Lett.* **2003**, *32*, 574–575; b) T. Soejima, N. Kimizuka, *Chem. Lett.* **2005**, *34*, 1234–1235; c) J. Zhu, Y. Shen, A. Xie, L. Qiu, Q. Zhang, S. Zhang, *J. Phys. Chem. C* **2007**, *111*, 7629–7633; d) A. Taubert, I. Arbell, A. Mecke, P. Graf, *Gold. Bull.* **2006**, *39*, 205–211.
[28] a) Z. H. Li, Z. M. Liu, J. L. Zhang, B. X. Han, J. M. Du, Y. A. Gao, T. Jiang, *J. Phys. Chem. B* **2005**, *109*, 14445–14448; b) M. Tsuji, M. Hashimoto, Y. Nishizawa, T. Tsuji, *Chem. Lett.* **2003**, *32*, 1114–1115.
[29] a) W. L. Huang, C. H. Chen, M. H. Huang, *J. Phys. Chem. C* **2007**, *111*, 2533; b) Z. R. Guo, Y. Zhang, Y. Q. Mao, L. Huang, N. Gu, *Mater. Lett.* **2006**, *60*, 3522–3525; c) J. P. Xie, J. Y. Lee, D. I. C. Wang, Y. P. Ting, *Small* **2007**, *3*, 672–682; d) J. H. Yuan, Z. J. Wang, Q. X. Zhang, D. X. Han, Y. J. Zhang, Y. F. Shen, L. Niu, *Nanotechnology* **2006**, *17*, 2641–2648; e) P. Jiang, J. J. Zhou, R. Li, Z. L. Wang, S. S. Xie, *Nanotechnology* **2006**, *17*, 3533–3538; f) P. Jiang, J. J. Zhou, R. Li, Y. Gao, T. L. Sun, X. W. Zhao, Y. J. Xiang, S. S. Xie, *J. Nanopart. Res.* **2006**, *8*, 927–934; g) L. Y. Wang, X. Chen, J. Zhan, Y. C. Chai, C. J. Yang, L. M. Xu, W. C. Zhuang, B. Jing, *J. Phys. Chem. B* **2005**, *109*, 3189–3194.
[30] During the preparation of the Au nanostructures at T = 90 °C, bmimPF_6 did hydrolyze, and small amounts of white solid were obtained [M. M. Jones, H. R. Clark, *Inorg. Chem.* **1971**, *10*, 28–33]. The white solid was removed by filtration with hot water and acetone. This phenomenon did not occur in bmimTf_2N.
[31] a) G. Li, M. Lauer, A. Schulz, C. Boettcher, F. Li, J. H. Fuhrhop, *Langmuir* **2003**, *19*, 6483–6491; b) N. Malikova, I. Pastoriza-Santos, M. Schierhorn, N. A. Kotov, L. M. Liz-Marzan, *Langmuir* **2002**, *18*, 3694–3697; c) Y. L. Luo, *Mater. Lett.* **2007**, *61*, 134–136; d) S. S. Shankar, A. Rai, A. Ahmad, M. Sastry, *Chem. Mater.* **2005**, *17*, 566–572; e) X. P. Sun, S. J. Dong, E. K. Wang, *Langmuir* **2005**, *21*, 4710–4712.
[32] R. C. Jin, Y. W. Cao, C. A. Mirkin, K. L. Kelly, G. C. Schatz, J. G. Zheng, *Science* **2001**, *294*, 1901–1903.
[33] H. M. J. Wang, I. J. B. Lin, *Organometallics* **1998**, *17*, 972–975.
[34] C. K. Lee, H. H. Peng, I. J. B. Lin, *Chem. Mater.* **2004**, *16*, 530–536.
[35] For distinct comparison, the molar ratio of $AuCl_4^-$/bmimPF_6 was increased to 1:2, and the solution was vacuum-dried completely to avoid the effect of water.
[36] J. D. Wadhawan, U. Schroder, A. Neudeck, *J. Electronal. Chem.* **2000**, *493*, 75–83.
[37] J. Dupont, S. M. Silva, R. F. de Souza, *Catal. Lett.* **2001**, *77*, 131–133.
[38] L. Chai, J. Klein, *Langmuir* **2007**, *23*, 7777–7783.
[39] G. T. Wei, Z. Yang, C. Y. Lee, H. Y. Yang, C. R. C. Wang, *J. Am. Chem. Soc.* **2004**, *126*, 5036–5037.
[40] C. C. Li, K. L. Shuford, Q. H. Park, W. P. Cai, Y. Li, E. J. Lee, S. O. Cho, *Angew. Chem. Int. Ed.* **2007**, *46*, 3264–3268.
[41] J. G. Zhang, Y. Gao, R. A. Alvarez-Puebla, J. M. Buriak, H. Fenniri, *Adv. Mater.* **2006**, *18*, 3233–3237.
[42] J. L. Zhang, J. M. Du, B. X. Han, Z. M. Liu, T. Jiang, Z. F. Zhang, *Angew. Chem. Int. Ed.* **2006**, *45*, 1116–1119.
[43] H. C. Chu, C. H. Kuo, M. H. Huang, *Inorg. Chem.* **2006**, *45*, 808–813.
[44] N. Tian, Z. Y. Zhou, S. G. Sun, Y. Ding, Z. L. Wang, *Science* **2007**, *316*, 732–735.
[45] G. S. Shafai, S. Shetty, S. Krishnamurty, V. Shah, D. G. Kanhere, *J. Chem. Phys.* **2007**, *126*, 014704.

Received: May 9, 2008
Published Online: July 16, 2008

